

RESEARCH ARTICLE

# Post-injury Inhibition of Endothelin-1 Dependent Renal Vasoregulation Mitigates Rhabdomyolysis-Induced Acute Kidney Injury

Jeremiah M. Afolabi , Pragalathan Kanthakumar, Jada D. Williams, Ravi Kumar, Hitesh Soni, Adebowale Adebisi\*

Department of Physiology, College of Medicine, University of Tennessee Health Science Center, Memphis, TN 38163, USA

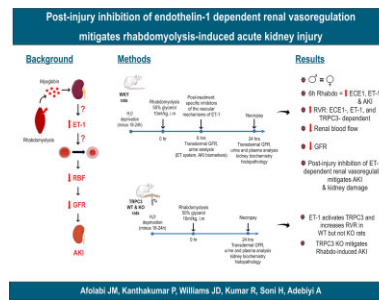
\*Address correspondence to A.A. (e-mail: [aadebiyi@uthsc.edu](mailto:aadebiyi@uthsc.edu))

## Abstract

In patients with rhabdomyolysis, the overwhelming release of myoglobin into the circulation is the primary cause of kidney injury. Myoglobin causes direct kidney injury as well as severe renal vasoconstriction. An increase in renal vascular resistance (RVR) results in renal blood flow (RBF) and glomerular filtration rate (GFR) reduction, tubular injury, and acute kidney injury (AKI). The mechanisms that underlie rhabdomyolysis-induced AKI are not fully understood but may involve the local production of vasoactive mediators in the kidney. Studies have shown that myoglobin stimulates endothelin-1 (ET-1) production in glomerular mesangial cells. Circulating ET-1 is also increased in rats subjected to glycerol-induced rhabdomyolysis. However, the upstream mechanisms of ET-1 production and downstream effectors of ET-1 actions in rhabdomyolysis-induced AKI remain unclear. Vasoactive ET-1 is generated by ET converting enzyme 1 (ECE-1)-induced proteolytic processing of inactive big ET to biologically active peptides. The downstream ion channel effectors of ET-1-induced vasoregulation include the transient receptor potential cation channel, subfamily C member 3 (TRPC3). This study demonstrates that glycerol-induced rhabdomyolysis in Wistar rats promotes ECE-1-dependent ET-1 production, RVR increase, GFR decrease, and AKI. Rhabdomyolysis-induced increases in RVR and AKI in the rats were attenuated by post-injury pharmacological inhibition of ECE-1, ET receptors, and TRPC3 channels. CRISPR/Cas9-mediated knockout of TRPC3 channels attenuated ET-1-induced renal vascular reactivity and rhabdomyolysis-induced AKI. These findings suggest that ECE-1-driven ET-1 production and downstream activation of TRPC3-dependent renal vasoconstriction contribute to rhabdomyolysis-induced AKI. Hence, post-injury inhibition of ET-1-mediated renal vasoregulation may provide therapeutic targets for rhabdomyolysis-induced AKI.

Submitted: 23 January 2023; Revised: 30 April 2023; Accepted: 1 May 2023

© The Author(s) 2023. Published by Oxford University Press on behalf of American Physiological Society. This is an Open Access article distributed under the terms of the Creative Commons Attribution-NonCommercial License (<https://creativecommons.org/licenses/by-nc/4.0/>), which permits non-commercial re-use, distribution, and reproduction in any medium, provided the original work is properly cited. For commercial re-use, please contact [journals.permissions@oup.com](mailto:journals.permissions@oup.com)



**Key words:** rhabdomyolysis; endothelin-1; TRPC3; renal vasoregulation; acute kidney injury

## Introduction

Acute kidney injury (AKI) is a sudden episode of kidney dysfunction that can also affect other organs<sup>1</sup>. Acute kidney injury occurs secondary to ischemia, hypoxia, or drug-induced nephrotoxicity, and it is the foremost kidney disease phenotype presented at clinics today.<sup>2</sup> What constitutes AKI has evolved over the years, but a consensus is that it shows a rapid decline in renal function and the buildup of nitrogenous waste products. Acute kidney injury is clinically diagnosed as a rise in creatinine by  $\geq 50\%$  from its baseline, a  $\geq 25\%$  decrease in glomerular filtration rate (GFR), and oliguria below 0.5 mL/kg/h for 6h, all in  $< 7$  d.<sup>3,4</sup> The AKI scale runs from initial risk through injury, failure, loss, and end-stage renal disease, aptly termed “RIFLE.”<sup>5</sup> Conservative estimates of the annual healthcare burden of hospital-acquired AKI alone on the United States healthcare system exceed \$10 billion.<sup>6</sup> Nevertheless, there are currently no effective therapies for AKI, partly due to late diagnosis and an incomplete understanding of disease pathophysiology.<sup>7</sup>

One of the causes of AKI is rhabdomyolysis. Rhabdomyolysis describes the rapid breakdown of injured skeletal muscle and the release of myoglobin into the circulation.<sup>8–10</sup> In theory, anything that causes muscle damage can trigger rhabdomyolysis. These include blunt trauma and crush injuries, drugs and toxins, alcohol abuse, exertional exercise, muscle ischemia, genetic defects, and certain infections.<sup>8</sup> Acute kidney injury is the most severe and life-threatening complication of rhabdomyolysis, with 10%–40% of patients developing some form of kidney insufficiency within days.<sup>11,12</sup> Experimental evidence points to myoglobin’s trifecta of roles: direct tubular injury, tubular obstruction via intratubular cast formation, and intrarenal vasoconstriction in the pathophysiology of rhabdomyolysis-induced AKI.<sup>10</sup> Of these three, renal vasoconstriction is the most injurious.<sup>13</sup> Persistent constriction of renal vessels in rhabdomyolysis results in severe ischemia<sup>9</sup> characterized by diminished renal blood flow (RBF) and GFR,<sup>8,13,14</sup> causing an abrupt decline in renal function.<sup>10</sup>

Increased renal production of vasoactive mediators likely contributes to the persistent vasoconstriction that reduces GFR. Indeed, rodents subjected to rhabdomyolysis exhibited increased plasma concentrations of endothelin (ET)-1, a potent renal vasoconstrictor.<sup>9,15</sup> A study has also demonstrated that rhabdomyolysis increased the density of endothelin receptors in the renal cortex and medulla.<sup>16</sup> Accumulation of myoglobin in the renal tubule generates reactive oxygen species (ROS).<sup>8</sup> Reactive oxygen species stimulates ET biosynthesis in various cell types.<sup>17,18</sup>  $H_2O_2$  transactivates the promoter of the endothelin converting enzyme (ECE-1), a peptidase that converts inactive big ET to the vasoactive isoform.<sup>19</sup> However,

the unanswered questions on the involvement of endothelin-1 (ET-1) in rhabdomyolysis-induced AKI include the unknown links between rhabdomyolysis and increased ET-1 production. The downstream effectors of ET-1-induced vasoconstriction are smooth muscle cell (SMC)  $Ca^{2+}$ -permeable ion channels, including the TRPC3 (transient receptor potential cation channel subfamily C member 3).<sup>20,21</sup> However, the ion channel mechanisms that trigger renal vasoconstriction in rhabdomyolysis remain unexplored. Since activation of G-protein-coupled receptors (GPCR) and ion channels regulate renal vascular resistance (RVR),<sup>22</sup> rhabdomyolysis may likely modulate RVR via GPCR and vascular ion channel mechanisms.

Most cases of rhabdomyolysis-induced AKI cannot be predicted. Hence, effective therapeutic interventions are those that can mitigate AKI after myoglobinuria has developed. It remains unclear whether post-injury inhibition of vascular ET-1 mechanisms ameliorates rhabdomyolysis-induced AKI. This study investigates the concept that ECE-1-driven ET-1 production in the kidney and ET-1-induced renal vascular SMC TRPC3 activation and resultant renal vasoconstriction contribute to rhabdomyolysis-induced AKI.

## Materials and Methods

### Animals

All experimental animal procedures were approved and performed following the guidelines of the Institutional Animal Care and Use Committee of the University of Tennessee Health Science Center. Male and female WKY (~120 g, 6-wk-old; Charles River); as well as male TRPC3 wild-type (WT) and knockout (KO) rats [Medical College of Wisconsin (MCW); Milwaukee, WI, USA] were used in this study. The TRPC3 mutant rats were generated by the Gene Editing Rat Resource Program (GERRC) at the MCW. This strain was created on the SS/JrHsdMcwi background by injecting a CRISPR targeting the exon 2 coding sequence AAAGGCTATGTGGCATCG into the rat embryos. A strain harboring a 25-bp frameshift mutation in exon 2 (rn6 chr2:123377980–123378004) was established by backcrossing to the parental strain and intercrossing to generate homozygous animals. Founder animals were genotyped by the Cel-1 assay and confirmed by Sanger sequencing. Fluorescent genotyping at the MCW confirmed the deletion. The rats were fed a regular low-salt diet (7912, Envigo Indianapolis, IN, USA).

Animals were assigned randomly to experimental groups. All rats were provided ad libitum access to food and water before and after the surgical procedures and were kept on a 12 h/12 h light/dark cycle during their housing in the vivarium.

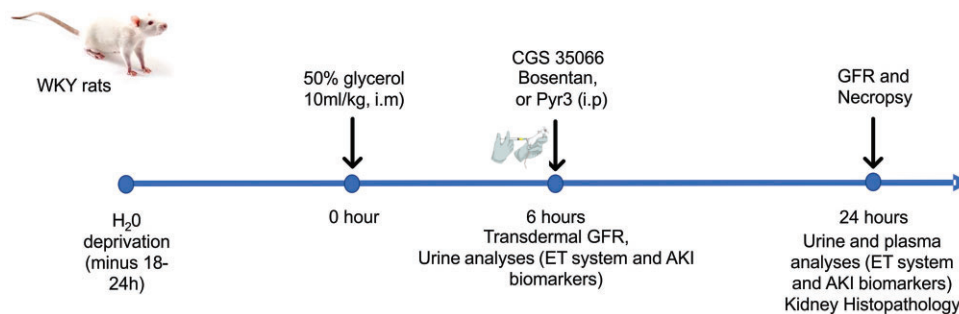


**Figure 1.** Experimental approach utilized to study the effect of post-injury inhibition of ET-mediated renal vasoregulation on rhabdomyolysis-induced AKI in rats. Rats were treated with CGS 35066 (30 mg/kg), bosentan (100 mg/kg), and pyr3 (10 mg/kg) 6 h after glycerol injection.

## Experimental Setup for Rhabdomyolysis Induction

Following ~24 h water deprivation, rats were placed in an isoflurane induction chamber and exposed to 5% isoflurane, which was subsequently reduced to 2% for maintenance. Upon confirmation of anesthesia, glycerol or vehicle (saline) was injected equally into both hindlimbs as follows: (10 mL/kg of glycerol diluted 1:2 in saline or 10 mL/kg of saline for control rats). The rats were allowed to recover for up to 24 h, after which the experiment was terminated.

## Treatment Protocol

As in other forms of AKI, prophylaxis offers little benefit to preventing rhabdomyolysis-induced AKI.<sup>23</sup> To examine the role of endothelin-dependent renal vasoregulation in mediating AKI following rhabdomyolysis, we subjected the animals to rhabdomyolysis and administered specific pharmacological agents 6 h after rhabdomyolysis had developed (Figure 1). Bosentan, a mixed ET<sub>A</sub>/ET<sub>B</sub> receptor antagonist at a dose of 100 mg/kg; CGS 35066, an ECE-1 inhibitor at a dose of 30 mg/kg; and Pyr3, a TRPC3 channel blocker at a dose of 10 mg/kg were administered intraperitoneally to the rats (Figure 1). The dose justification for the inhibitors was based on previous studies.<sup>24–26</sup>

## Glomerular Filtration Rate Determination

As previously described,<sup>27–29</sup> the three-compartment method with FITC-sinistrin clearance was used to determine GFR. Briefly, a predetermined region on the flank was shaved, and a depilatory cream was applied to remove residual fur. The optical transdermal GFR device (MediBeacon GmbH, Mannheim, Germany) was prepared, and the battery was attached. Using a dual-sided adhesive patch, the device was attached to the skin surface of the rats and held in place with an elastic gauze bandage. The device was left for ~3 min to record a steady background. A warm compress was applied to the tail to dilate the veins in preparation for intravenous injection of FITC-sinistrin in sterile saline (50 mg/mL) at (5 mg/100 g b. wt). Once the baseline was sufficiently acquired, FITC-sinistrin was administered in a smooth, rapid bolus. The device was left alone for ~2 h to record FITC-sinistrin clearance. The device was removed at the end of the acquisition, and the data were analyzed following the manufacturer's instructions using the MediBeacon Studio 3 software.

## Measurement of Arterial Blood Pressure in Conscious Rats

The easyTEL + M1.PTA transmitters (emka Technologies, Paris, France) were used to measure blood pressure and heart rate in

conscious TRPC3 WT and KO rats. The rats were anesthetized with ketamine (100 mg/kg) and xylazine (10 mg/kg) administered intraperitoneally. Buprenorphine (0.05 mg/kg; sustained release) was administered subcutaneously to all animals to reduce pain. A pressure-sensing catheter was inserted via the carotid artery, and the body of the transmitter was implanted in a subcutaneous pouch on the left flank. Five days post-surgery, blood pressure and heart rate readings were sampled every 10 s for 24 h. Post-collection data was analyzed using the vendor's software.

## Sample Collection

Blood was collected from the retroorbital sinus into heparin tubes. The tubes were subsequently centrifuged, and the plasma was collected and stored for analysis. Urine specimens were collected from individual rats as previously described.<sup>30,31</sup> Briefly, individual rats were weighed and placed on a 96-well plate inside an empty 5 mL pipette tip box for ~2 h. Urine samples were then collected from the wells, centrifuged, and analyzed. The kidneys were sectioned transversely and stored in 4% buffered formalin for histopathological analysis or frozen in a freezer (-80°C).

## Biochemical Assays

Urine myoglobin levels were determined using the Rat myoglobin kit from Abcam (Ab157739; Boston, MA, USA). Lipocalin-2 (NGAL; 80687) was quantified with rat-specific ELISA kits purchased from Crystal Chem (Elk Grove Village, IL, USA). BUN concentrations were determined using the IDEXX Catalyst BUN kit (98-11070-01) on a Catalyst One veterinary chemistry analyzer (Westbrook, ME, USA). Urine levels of ECE-1 and ET-1 were determined using isoform-specific rat ELISA kits from MyBioSource (ECE-1 MBS2885758; San Diego, CA, USA) and Reddot Biotech (RDR-EDN1-RA; Kelowna, BC, Canada), respectively. The kits were used following the manufacturer's instructions. Urinary markers were normalized to urinary creatinine to control for urine flow rate and creatinine clearance variations. Liquid chromatography-tandem mass spectrometry was used to determine creatinine concentrations at the UAB/UCSD O'Brien Core Center for AKI Research at the University of Alabama at Birmingham.

## Histopathology

Histopathological analysis was performed independently by Probetex (San Antonio, TX, USA). Kidney samples were fixed in 4% neutral-buffered formalin, dehydrated in graded alcohols, and embedded in paraffin. The samples were then sectioned

**Table 1:** Oligonucleotide primer sequences.

Gene	Sequence	Accession	Length (bp)
qRT-PCR: TRPC3			
Forward	5'—CATCAGCAAAGGCTATGTGCG—3'	NM.021771.2	111
Reverse	5'—TCGTTCATCGCGCAGTTCTT—3'		
GAPDH			
Forward	5'—AGTGCCAGCCTCGTCTCATA—3'	XM.032905640.1	100
Reverse	5'—TTGTCAACAAGAGAAGGCAGC—3'		

for hematoxylin and eosin (H&E) staining. Sections were examined for morphological damage, including dilated tubules, protein casts, and tubular necrosis. The slides were randomly intermixed and scored blinded: 0 absent, 1+ minimal or rare focal, 2+ mild, 3+ moderate, and 4+ marked.

### Tissue Preparation and Wire Myography

Animals were euthanized by exsanguination under isoflurane anesthesia. Renal arteries were harvested in ice-cold modified Krebs's solution (MKS; 134 mM NaCl, 6 mM KCl, 2.0 mM CaCl<sub>2</sub>, 2 mM MgCl<sub>2</sub>, 10 mM HEPES, and 10 mM glucose, pH 7.4). After gently removing connective tissue and fat, ~2 mm segments of the main renal arteries were mounted in a small vessel wire myograph chamber (model 620M; Danish Myo Technology, Aarhus, Denmark) for isometric tension recording.<sup>32–35</sup> Two steel wires (40 μm diameter) were passed through the arterial lumen and mounted onto the myograph jaws. The vessels were allowed to equilibrate in the oxygenated MKS solution at 37°C and pH 7.4 and then stretched to their optimal lumen diameter for active tension development. The internal circumference/wall tension ratio of the renal artery segments was computed by setting the internal circumference, L1, to 90% of a value established by a passive tension equivalent to a transmural pressure of 100 mmHg. Using the equation  $I1 = L1/\pi$ , the diameter of the arteries was subsequently calculated (DMT Normalization Module; ADInstruments, Sydney, Australia). Following a 1-h equilibration period, baseline recordings and changes in isometric tension following ET-1 (10 mM) addition were documented in the absence and presence of Pyr3 (20 mM). Data were recorded and analyzed using LabChart 8 (ADInstruments, Dunedin, New Zealand).

### Isolation of Smooth Muscle Cells

Renal vascular SMCs were isolated from renal arteries using a HEPES-buffered isolation solution containing the following (in mM): 134 NaCl, 6 KCl, 1 MgCl<sub>2</sub>, 10 HEPES, and 10 glucose (pH 7.4). The arteries were incubated in an isolation solution containing the following (in mg/mL): 1 mg/mL papain, 1 mg/mL dithioerythritol, and 1 mg/mL BSA for 1614 min at 37°C. Arteries were then incubated in an isolation solution containing the following: 0.5 mg/mL liberase blendzyme, 1 mg/mL collagenase F, 0.5 mg/mL collagenase H, 100 μM CaCl<sub>2</sub>, and 1 mg/mL BSA, 1 mg/mL BSA, and 100 nM CaCl<sub>2</sub> for 87 min at 37°C. Digested vessels were washed in isolation and triturated using fire-polished glass Pasteur pipettes to yield single SMCs.

### Patch-clamp Electrophysiology

Whole-cell currents were recorded in a conventional whole-cell patch-clamp configuration. Patch electrodes were pulled

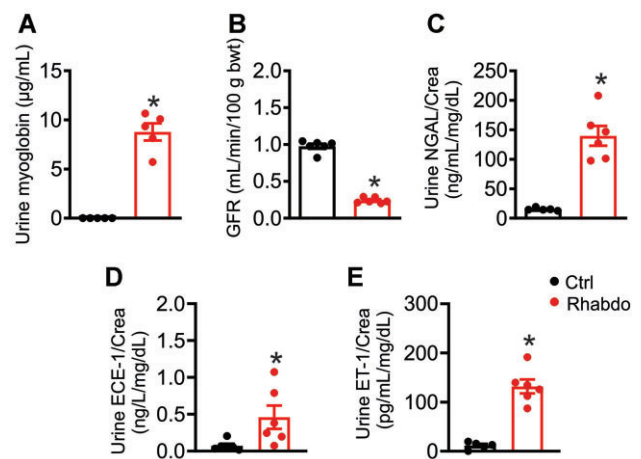


**Figure 2.** Glycerol-induced rhabdomyolysis causes AKI and increases renal ECE-1 and ET-1 production in male Wistar rats at 6 h. Urine myoglobin (A) levels in saline (Ctrl)- and glycerol (Rhabdo)-treated rats ( $n = 5$ ). (B) and (C) GFR and urine NGAL in Ctrl and Rhabdo rats ( $n = 6$ ). (D) and (E) Urine ECE-1 and ET-1 levels in Ctrl and Rhabdo rats ( $n = 6$ ). \* $P < 0.05$  vs. Ctrl (unpaired t-test).

from Borosilicate glass tubes using a P-1000 Flaming/Brown micropipette puller (Sutter Instrument, Novato, CA, USA) and fire polished using a microforge (Narishge, MF-830) to reach a resistance of 3–6 MΩ. Cells were placed in a bath solution with the following composition: (in mM) NaCl 140, MgCl<sub>2</sub> 1.2, CaCl<sub>2</sub> 1.8, HEPES 10, glucose 10, pH 7.4 (using 1 M NaOH). The pipette solution used had the following composition: (in mM) CsCl 140, MgCl<sub>2</sub> 2, HEPES 10, EGTA 5, glucose 10, Na-ATP 5, pH 7.35 (using 1 M CsOH). All data were acquired and digitized using Axopatch 200B patch clamp amplifier, Axon Instruments Digidata 1550B analog-digital converter, and pClamp 10 acquisition software (Molecular Devices, CA, USA). Data were sampled at 10 kHz, filtered at 2 kHz (low-pass Bessel filter), and sampled at 20 kHz. Membrane currents were recorded by applying 940-ms voltage ramps from –120 to +30 mV. Using a voltage clamp protocol, the command voltage ramped up from –100 to +100 mV over 940 ms from a zero-mV holding potential.

### Renal Hemodynamics Measurement

To administer ET-1 directly into the kidney, a catheter was inserted in the left femoral artery and advanced through the abdominal aorta until its tip was positioned at the junction of the aorta and left renal artery. The catheter was connected to a flow pump, which delivered ET-1 at a flow rate of 10 ng/kg/min for ~30 min. Flank incisions provided access to the renal pedicles. The left kidney was exposed retroperitoneally. Total RBF was measured with a flow probe (Transonic Systems,

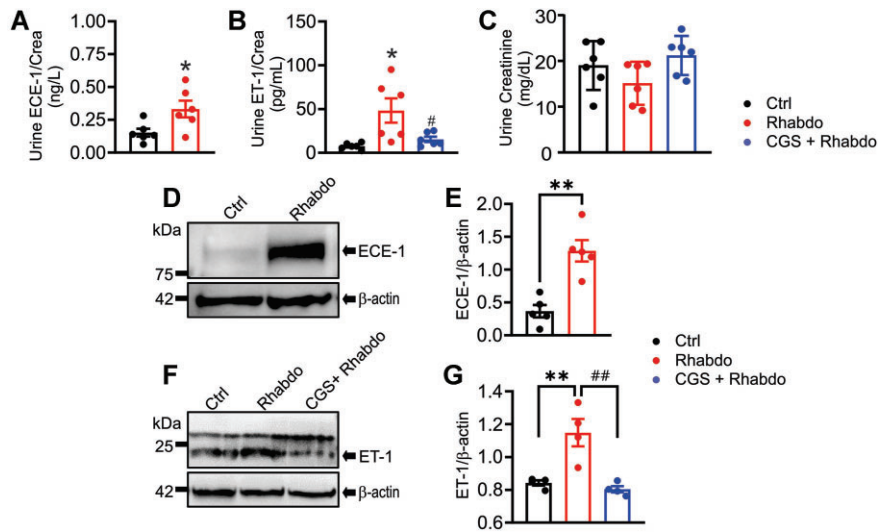


**Figure 3.** Twenty-four-hour rhabdomyolysis increases renal ECE-1 and ET-1 levels in male Wistar rats. (A–C) Urine ECE-1, ET-1, and creatinine levels in saline (Ctrl)- and glycerol (Rhabdo)-treated rats ( $n = 6$ ). (D–G) Western blots of ECE-1 and ET-1 (in the absence and presence of 30 mg/kg CGS 35066) in kidneys from Ctrl and Rhabdo rats (ECE1,  $n = 5$ ; ET-1,  $n = 4$ ). CGS 35066: ECE-1 inhibitor. \* $P < 0.05$  vs. Ctrl; # $P < 0.05$  vs. Rhabdo [unpaired t-test (A and D); one-way ANOVA, with Holm–Šidák’s post hoc test, (B, C, and F)].

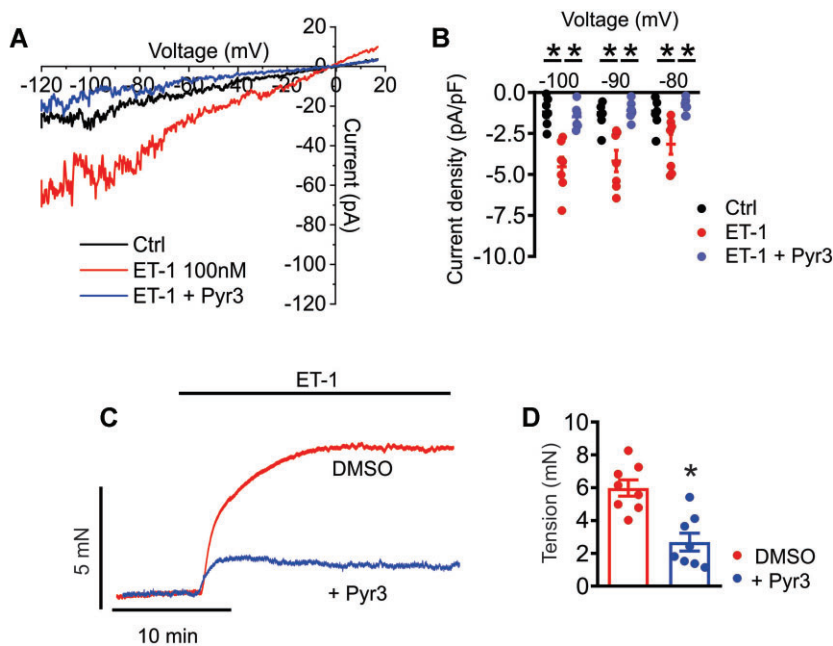


**Figure 4.** Pyr3 inhibits ET-1-induced cation currents in renal vascular SMCs and the contraction of renal arteries. (A) and (B) Representative tracings and graphs showing ET-1 (100 nM)-induced cation currents in renal vascular SMCs (isolated from 4 rats each) in the absence and presence of the TRPC3 channel blocker pyr3 (10  $\mu$ M). (C) and (D) Representative tracings and bar charts showing ET-1 (10 nM)-induced renal artery contraction in the absence and presence of pyr3 (20  $\mu$ M) ( $n = 8$ ). \* $P < 0.05$  vs. ET-1 [one-way ANOVA, with Holm–Šidák’s post hoc test, (B); unpaired t-test (D)].

Ithaca, NY, USA) placed around the main renal artery and connected to a flowmeter (Transonic Systems). Renal cortical perfusion and mean arterial pressure (MAP) were recorded using a Laser-Doppler probe (Perimed, Jarfalla, Sweden) and physiological pressure transducer (ADInstruments, Colorado Springs, CO, USA) systems, respectively. All recordings were acquired simultaneously using the PowerLab data acquisition system and LabChart Pro software.

### Quantitative RT-PCR

Total RNA was isolated with the Direct-zol RNA Miniprep Plus kit (Zymo Research; Irvine, CA, USA). A high-capacity cDNA reverse transcription kit (Life Technologies; Grand Island, NY, USA) was used to synthesize cDNAs from the RNA samples. Quantitative RT-PCR (qRT-PCR) was performed in the QuantStudio System using an Applied Biosystems SYBR Green Master Mix

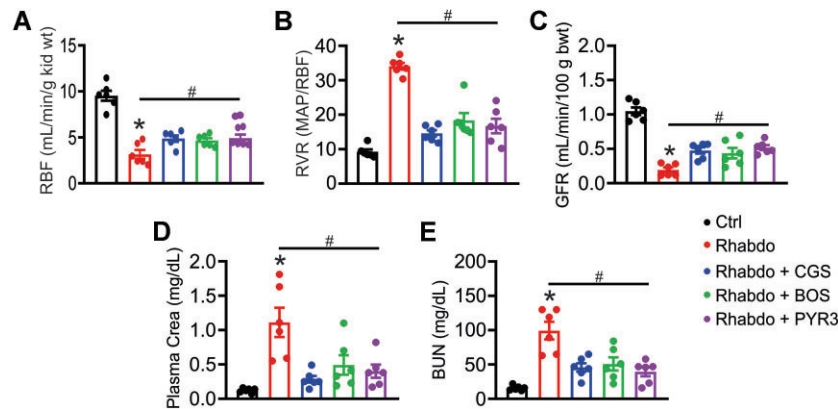


**Figure 5.** Post-injury inhibition of the ET system mitigates rhabdomyolysis-induced reduction in RBF and AKI. (A) and (B) Charts summarizing RBF and RVR in saline (Ctrl)- and glycerol (Rhabdo)-treated rats ( $n = 6$ ); (C–E) GFR, plasma creatinine, and BUN in Ctrl and Rhabdo (in the absence and presence of inhibitors) rats ( $n = 6$ ). \* $P < 0.05$  vs. Ctrl; # $P < 0.05$  vs. Rhabdo (one-way ANOVA, with Holm–Šidák’s post hoc test). CGS (CGS 35066); BOS (bosentan).

kit (Life Technologies). Gene expression levels were normalized to GAPDH as the internal control. The gene-specific oligonucleotide primers used are listed in Table 1.

### Western Immunoblotting

Protein lysates were isolated from representative kidney tissues using RIPA lysis buffer and denatured (using LDS sample buffer + DTT and heated at 70°C for 10 min). Approximately 50  $\mu$ g protein was subsequently loaded onto polyacrylamide gels for size fractionation in a Mini Trans-Blot Cell (Bio-Rad) and transferred onto PVDF membranes using a semi-dry blotter. Once the transfer was completed, the membranes were blocked for ~1 h using Tris-buffered saline supplemented with 0.05% Tween (TBS-T) and 2% BSA. The membranes were then incubated with the respective primary antibodies overnight at 4°C. After a wash in TBS-T, the membranes were incubated in HRP-conjugated secondary antibodies for 45 min at room temperature. Immunoreactive proteins were visualized using a chemiluminescent reagent.

### Antibodies and Reagents

Rabbit polyclonal anti-ECE1 (Life Technologies, Grand Island, NY, USA; PA5-81948) and rabbit polyclonal anti-ET-1 (Protein-tech, Rosemont, IL, USA; 12191-1-AP) were used at 1:200 dilutions, while rabbit monoclonal anti-beta actin (Abcam, Cambridge, MA, USA; MA515739) was used at 1:1000 dilutions. Anti-rabbit secondary antibody (Abcam, Cambridge, MA, USA; ab6721) was used at 1:10000 dilutions. Unless otherwise specified, all reagents were purchased from Sigma-Aldrich (St. Louis, MO, USA). CGS 35066 was purchased from Bio-Techne (Minneapolis, MN, USA) and Bosentan from Cayman Chemical; Ann Arbor, MI, USA). Liberase blendzyme was purchased from Roche Life Science (Indianapolis, IN, USA).

### Statistical Analysis

Data are presented as means  $\pm$  SE. Statistical analysis was performed with Graph Pad software (Sacramento, CA, USA). Student’s t-test and ANOVA (followed by the Holm–Šidák or Tukey’s post hoc test) were used. Statistical significance implies a  $P < 0.05$ .

## Results

### Rhabdomyolysis Causes Kidney Injury and Increases Renal ECE-1 and ET-1 Production in Male Wistar Rats

Rhabdomyolysis causes myoglobinuria.<sup>36</sup> Myoglobin was present in the urine 6 h after glycerol injection (Figure 2A). This correlated with kidney injury evidenced by reduced GFR and elevation in the early AKI biomarker, urinary NGAL (Figures 2B and C). Correspondingly, the urinary levels of ECE-1 and ET-1 were increased in glycerol-treated rats (Figures 2D and E). At 24 h, the increase in urinary ECE-1 and ET-1 was sustained in glycerol-treated rats (Figure 3A and B). These increases in urinary ECE-1 and ET-1 were not driven by changes in urine creatinine concentration (Figure 3C). Western blot analyses demonstrated an increase in ECE-1 and ET-1 protein expressions in kidney tissues of rats 24 h after glycerol injection. (Figures 3D–G). Treatment of the rats with CGS 35066, an ECE-1 inhibitor, reversed the glycerol-induced increase in urinary and kidney tissue ET-1 (Figures 3B, F, and G).

### Endothelin Activates TRPC3 Channels in Renal VSMCs

Downstream of ET-induced vascular reactivity is TRPC3-mediated  $Ca^{2+}$  signaling.<sup>20,21</sup> Data here show ET-1 evoked strong inward cation currents in isolated rat renal vascular SMCs at several voltages (Figures 4A and B). Similarly, ET-1-induced significant contraction of isolated renal arteries (Figures 4C and D). Cation currents and contraction engendered by ET-1 were attenuated by Pyr3, a TRPC3 channel blocker (Figures 4A–D).

### Rhabdomyolysis-induced ET Production Reduces RBF By Activating ET Receptors and TRPC3 Channels

Acute kidney injury occurred 6 h after glycerol injection (Figures 2B and C). To investigate whether rhabdomyolysis-induced ET production reduces RBF by activating ET receptors and TRPC3 channels, rats were treated with pharmacological inhibitors of ECE-1 (CGS 35066), ET receptors (bosentan), or TRPC3 channels (Pyr3) 6 h after glycerol injections (Figure 1). Renal blood flow was significantly reduced, and RVR increased in glycerol-treated rats (Figures 5A and B). Glycerol-induced changes in these indices were diminished by CGS 35066, bosentan, and Pyr3 (Figures 5A and B).

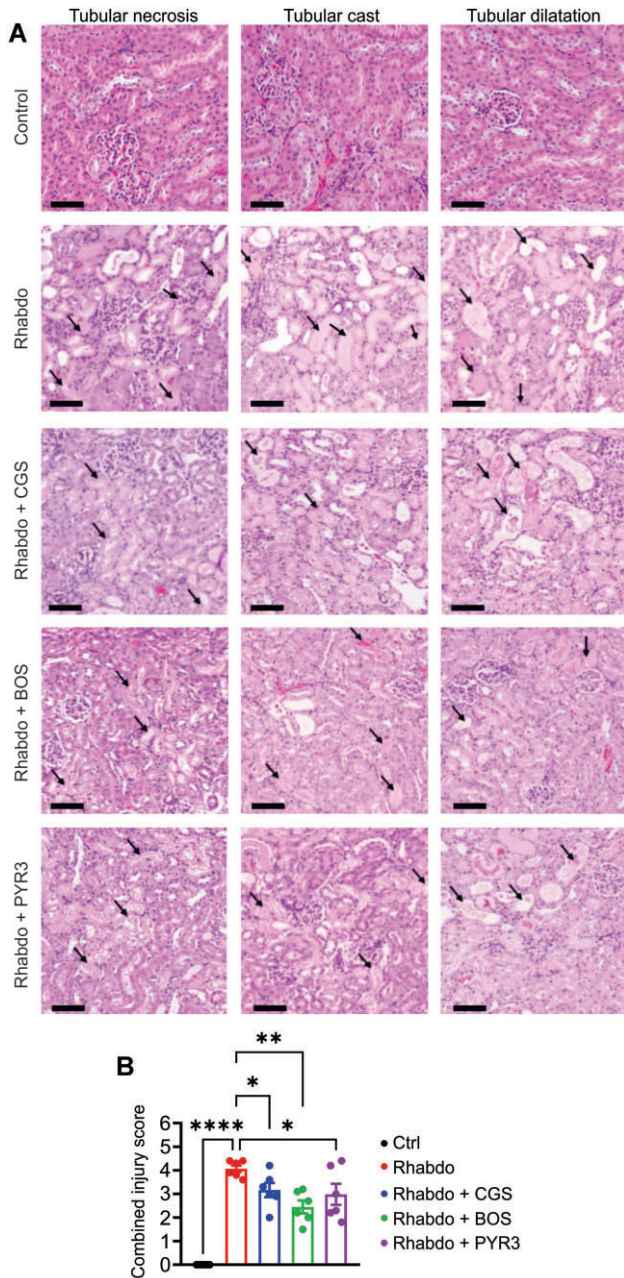


**Figure 6.** Histopathology indicates that post-injury inhibition of the ET system attenuates rhabdomyolysis-induced kidney damage. (A) Hematoxylin and eosin staining of kidney sections (arrows indicate tubular injury), and (B) combined injury score in Ctrl and Rhabdo in the absence and presence of inhibitors ( $n = 6$ ). CGS: CGS 35066 (30 mg/kg), ECE-1 inhibitor; BOS: Bosentan (100 mg/kg), ET-receptor antagonist; PYR3: 10 mg/kg, TRPC3 channel blocker. \* $P < 0.05$  (one-way ANOVA, with Holm-Šidák's post hoc test); bar = 100  $\mu\text{m}$ .

### Post-injury Inhibition of the Vascular Mechanisms of ET-1 Mitigates AKI and Morphological Kidney Damage

Like RBF and RVR, administration of CGS 35066, bosentan, and Pyr3 6 h after glycerol injection reduced GFR, plasma creatinine, and BUN alterations (Figures 5C–E). These inhibitors also attenuated glycerol-induced morphological kidney damage (Figures 6A and B).

### Genetic Ablation of TRPC3 Channels Does Not Cause Basal Kidney Injury in Rats

TRPC3 mutant rats were used to support the pharmacological inhibition of TRPC3. qPCR confirmed amplification of TRPC3 in WT but not KO kidney samples (Figures 7A and B). Day and night arterial pressure and heart rate were unaltered in WT versus KO rats (Figures 7C–E). Baseline kidney function (GFR and plasma creatinine) was also unchanged in the rats (Figures 7F and G).

### Endothelin-1-induced Activation of TRPC3 Channels, MAP Elevation, and Decreases in Renal Perfusion Are Reversed in TRPC3 KO Rats

Endothelin-1-induced cation currents in renal vascular SMC of WT rats (Figures 8A and B). By contrast, ET-induced cation currents were abolished in KO rat renal vascular SMC (Figures 8C and D). Similarly, ET-1-induced contraction of renal arteries was diminished in the KO rats (Figures 8E and F). Renal hypoperfusion (decreased cortical perfusion and RBF) and MAP and RVR increases elicited by direct renal artery infusion of ET-1 were essentially abrogated in KO rats (Figures 8G–I).

### TRPC3 KO Mitigates Rhabdomyolysis-Induced AKI

To explore whether the KO of TRPC3 channels protects against rhabdomyolysis-induced AKI, TRPC3 WT and KO rats were subjected to glycerol-induced rhabdomyolysis. Twenty-four-hour rhabdomyolysis led to comparable increases in urinary ET-1 production in WT and KO rats (Figure 9A). However, rhabdomyolysis-induced reduction in GFR and elevations in BUN and plasma creatinine were all attenuated in the KO rats (Figures 9B–D). Similarly, rhabdomyolysis-induced morphological kidney damage was diminished in the KO rats (Figures 9E and F). Statistically, we found interactions between TRPC3 gene KO (row factor) and glycerol treatment/rhabdomyolysis (column factor),  $P = < 0.0001, 0.0002, < 0.0001$  for BUN, plasma creatinine, and histopathology data, suggesting an influence of gene KO on the effect of glycerol. The effect of gene KO was not significant in ET-1 production but was significant in other measures:  $P = 0.0049, < 0.0001, 0.0002, \text{ and } < 0.0001$  for GFR, BUN, plasma creatinine, and histopathology data, respectively, suggesting an influence for gene KO on the degree of AKI following glycerol injection. The effect of rhabdomyolysis was highly significant ( $P = < 0.0001$ ) in all measures evaluated.

### Glycerol-induced Rhabdomyolysis Is Not Sex-Dependent

We explored sex differences in rhabdomyolysis and the associated kidney injury. Both males and females exhibited comparable myoglobinuria 24 h after glycerol injection (Figure 10A). Glycerol-induced GFR decrease was similar in male and female rats (Figure 10B). Other markers of AKI show the same trend, with significant increases in plasma creatinine and blood urea nitrogen (BUN) in both sexes (Figures 10C and D). No interaction was found between sex and glycerol treatment,  $P = 0.95, 0.261, 0.722, \text{ and } 0.458$  for urine myoglobin, GFR, plasma creatinine, and BUN, respectively. The effect of sex is not significant with  $P = 0.913, 0.329, 0.696, \text{ and } 0.518$  for urine myoglobin, GFR, plasma creatinine, and BUN, respectively. The effect of rhabdomyolysis was significant, with  $P = 0.0007$  for urine myoglobin and  $P < 0.0001$  for GFR, plasma creatinine, and BUN. Histological analyses indicated comparable tubular necrosis, dilatation, and

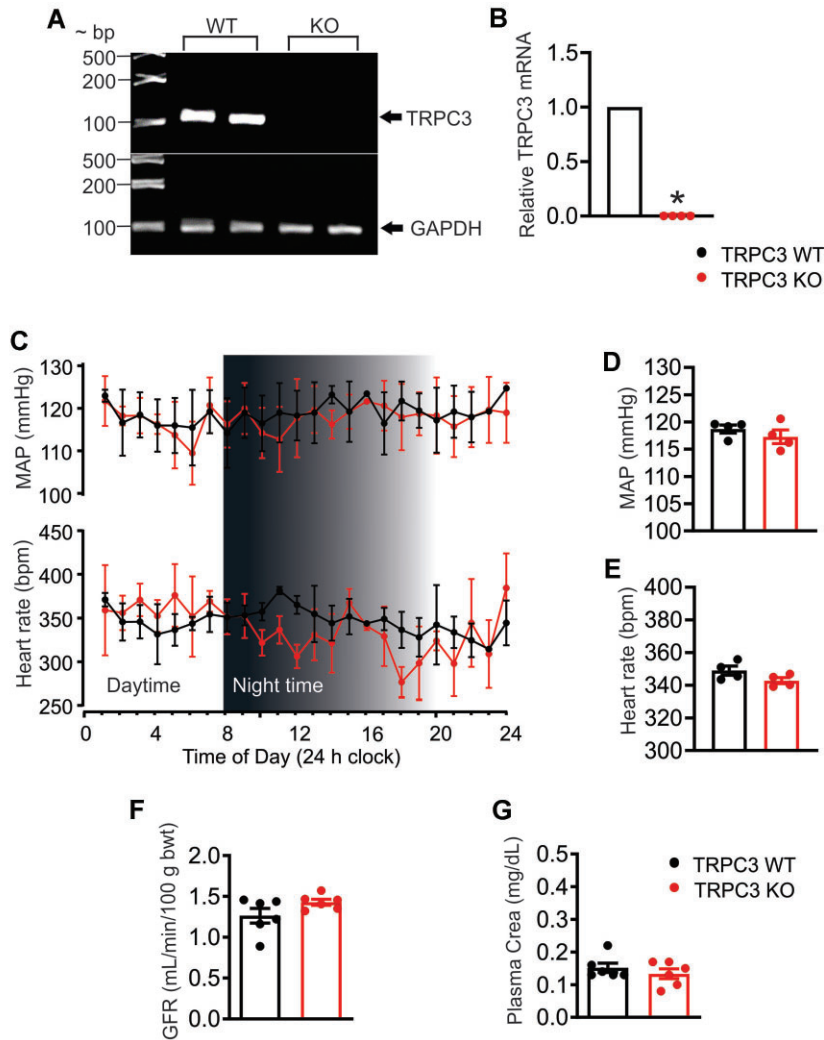


**Figure 7.** Baseline vascular and kidney functions are unaltered in TRPC3 mutant rats (SS background). (A) and (B) Gel image and qPCR showing the absence of TRPC3 in the mutant rats. (C–E) Day and night recordings, as well as average MAP and heart rate in TRPC3 WT and KO rats ( $n = 4$ ). Average GFR (F), and plasma creatinine (G) in TRPC3 WT and KO rats ( $n = 6$ ). \* $P < 0.05$  vs. TRPC3 WT (unpaired  $t$ -test).

cast formation in glycerol-treated male and female rats (Figures 11A and B).

## Discussion

This paper examined previously unexplored concepts, including renal ECE-1 generation and subsequent ET-1 production in rhabdomyolysis, the involvement of vascular SMC TRPC3 channels in rhabdomyolysis-induced AKI, and post-injury amelioration of rhabdomyolysis-induced AKI by inhibition of ET-1-dependent vasoregulation. Findings suggest that: (1) rhabdomyolysis stimulates renal ECE-1-dependent ET-1 production; (2) TRPC3 mediates ET-induced renal artery contraction; (3) post-injury inhibition of ET-1 biosynthesis and TRPC3 channels ameliorate rhabdomyolysis-induced AKI; and (4) the severity of glycerol-induced AKI in male and female rats is comparable.

Rapid vasoconstriction of pre- and post-glomerular vessels leading to a significant reduction in RBF and GFR are critical factors in glycerol-mediated renal insufficiency.<sup>37,38</sup> Kidney injury severity increases with the RBF decline.<sup>39</sup> Here, rhabdomyolysis-induced AKI in glycerol-treated rats correlated with RBF reduction and RVR increase, supporting the concept

of persistent renal vasoconstriction caused by kidney accumulation of myoglobin. Increased production of ET-1, a potent vasoconstrictor, has been demonstrated in myoglobin-treated glomerular mesangial cells and the plasma of rats subjected to glycerol-induced rhabdomyolysis.<sup>9</sup> However, this study is the first to show that a rhabdomyolysis-induced increase in ET-1 level depends on an upstream increase in protease ECE-1. In addition to renal vascular endothelial cells, tubular epithelial cells are a significant source of renal endothelin synthesis.<sup>40–42</sup> Zager and colleagues showed that within 24 h of unilateral renal ischemia-reperfusion injury, kidney cortex ET-1 mRNA was elevated 4-fold and, in two weeks, increased to >10-fold compared to non-ischemic kidneys.<sup>43</sup> We speculate that tubular cells, especially those of the proximal tubule and the collecting duct, play a role in endothelin-mediated AKI. Increased vascular endothelial and tubular ET-1 production in rhabdomyolysis may cause vasoconstriction, a subsequent reduction in GFR, and associated AKI.

Since urinary ET-1 is mainly of renal origin,<sup>44,45</sup> we measured urinary ECE-1 and ET-1 levels in rats subjected to rhabdomyolysis. Increased renal production of ECE-1 and ET-1 occurs as early as 6 h after glycerol injection, sustained up to 24 h,

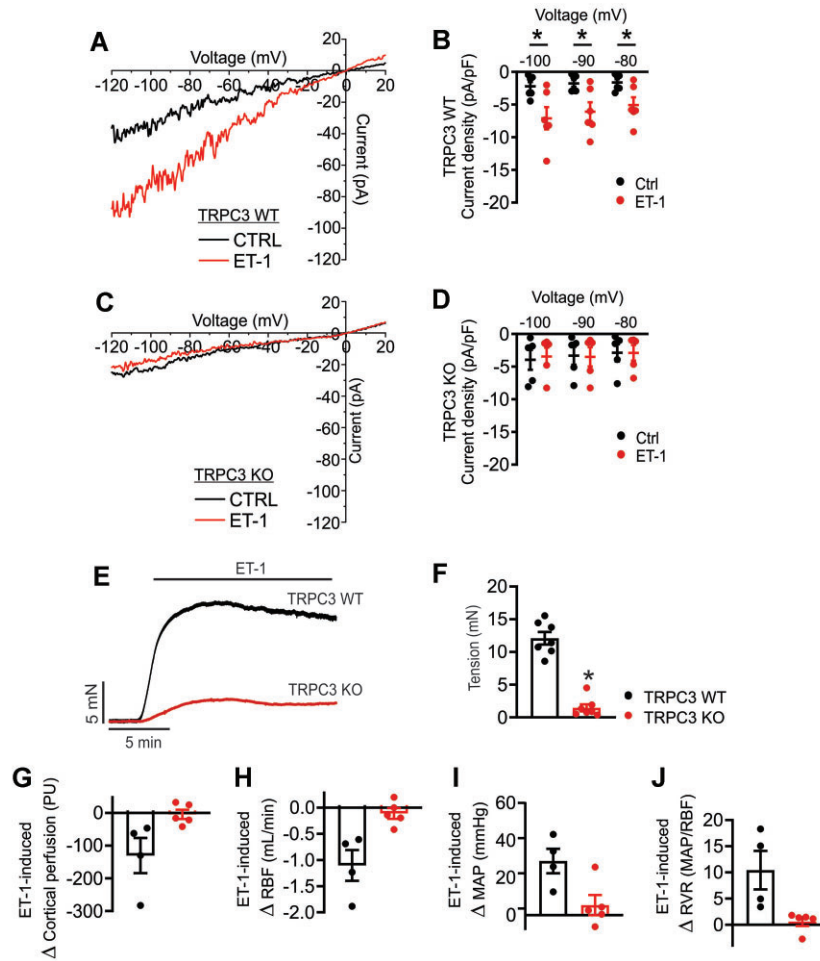


**Figure 8.** Endothelin-1-induced cation currents, renal artery contraction, kidney hypoperfusion, and MAP increase are lessened in TRPC3 KO rats. (A–D) Representative tracings and graphs showing ET-1 (100 nM)-induced cation currents in SMCs isolated from TRPC3 WT and KO rat renal arteries ( $n = 3$  animals each). (E) and (F) Tracings and bar charts showing ET-1 (10 nM)-induced contraction in TRPC3 WT and KO rat renal arteries ( $n = 7$ ). (G–J) Charts illustrating ET-1 (10 ng/kg/min) effects on renal cortical perfusion, RBF, MAP, and RVR in TRPC3 WT ( $n = 4$ ) and KO rats ( $n = 5$ ). \* $P < 0.05$  vs. ET-1/TRPC3 WT (unpaired t-test).

and is associated with AKI. Inhibiting ECE-1 reduced renal ET-1 production and mitigated AKI. These data suggest that myoglobin is a robust stimulant of ECE-1-dependent ET-1 biosynthesis in the kidney. Myoglobin causes oxidative stress via the accumulation of oxyradicals in the kidney.<sup>8,46</sup> Reactive oxygen species are a potent driver of ET generation.<sup>17,47</sup> Treatment of renal epithelial cells with H<sub>2</sub>O<sub>2</sub> generator glucose oxidase increased ECE-1-dependent cellular ET production.<sup>42</sup> Conceivably, ROS is the link between myoglobin and renal ET biosynthesis. However, ET itself can generate ROS,<sup>17</sup> indicating the central role of ROS in the vicious cycle of the renal pathophysiology of ET.

Endothelin receptors ET<sub>A</sub> and ET<sub>B</sub> are coupled to G-proteins and, when activated by ET, trigger a cascade of events that control intracellular Ca<sup>2+</sup> levels and vascular reactivity.<sup>48–50</sup> G-protein-coupled receptor activation initiates phosphoinositide hydrolysis, resulting in inositol triphosphate (IP<sub>3</sub>) and diacylglycerol (DAG).<sup>51</sup> Inositol triphosphate subsequently binds to receptors on the sarcoplasmic reticulum (SR) to facilitate Ca<sup>2+</sup> release from the SR Ca<sup>2+</sup> store. Depleting Ca<sup>2+</sup> from the SR store triggers extracellular Ca<sup>2+</sup> influx via store-operated Ca<sup>2+</sup> channels.<sup>52–54</sup> Diacylglycerol can increase intracellular Ca<sup>2+</sup> independent of store-operated channels, as it activates receptor-operated Ca<sup>2+</sup> channels on the plasma membrane, resulting in

channel opening and Ca<sup>2+</sup> influx.<sup>53,55</sup> Both store- and receptor-operated channels are known to include the TRPC channels.<sup>55,56</sup> TRPC proteins constitute a family of seven (TRPC1–7) nonselective cation channels, but only TRPC 1, 3, 4, 5, and 6 are expressed in rat renal vessels.<sup>57</sup> Of the lot, TRPC3 is predominant.<sup>57</sup> Endothelin-1 activates TRPC3 in the cerebral and mesenteric arteries.<sup>20,21</sup> A recent study demonstrated that ET stimulates receptor-operated Ca<sup>2+</sup> entry via TRPC3 in swine renal microvessels.<sup>42</sup> Findings here show that the TRPC3 blocker Pyr3 diminished ET-1-induced cation currents in renal vascular SMCs. Similarly, Pyr3 blunted ET-1-induced renal arteries contraction, consistent with a previous study in rat mesenteric arteries.<sup>20</sup>

Rhabdomyolysis cannot reasonably be predicted. Therefore, studies on prophylactic intervention may have limited clinical significance. Thus, the importance of this study includes the findings that pharmacological interventions that target ET biosynthesis and downstream mechanisms of vascular reactivity attenuated AKI after rhabdomyolysis had developed. Intraarterial infusion of CGS 35066, a selective ECE-1 inhibitor at 30 mg/kg alongside an angiotensin-converting enzyme (ACE) inhibitor, decreased MAP in spontaneously hypertensive rats, suggesting a synergy between the ET system and the renin-angiotensin system in maintaining blood pressure.<sup>58</sup> Similarly,

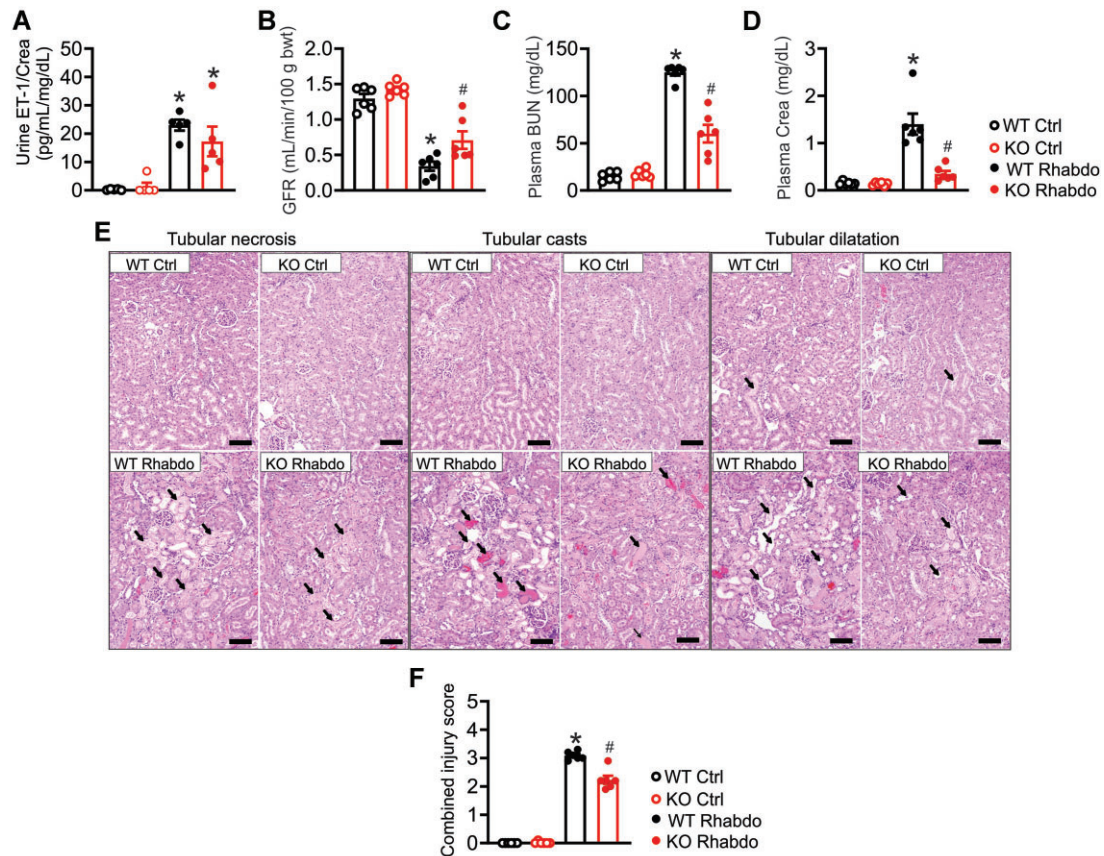


**Figure 9.** Genetic ablation of TRPC3 channels mitigates rhabdomyolysis-induced AKI. Urine ET-1 (A) levels in saline (Ctrl)- and glycerol (Rhabdo)-treated TRPC3 WT and KO rats ( $n = 5$ ). Glomerular filtration rate (B), BUN (C), and plasma creatinine (D) in TRPC3 WT and KO Ctrl and Rhabdo rats ( $n = 6$ ). (E and F) Staining of kidney sections (arrows indicate tubular injury), and combined injury score in Ctrl and Rhabdo TRPC3 WT and KO rats ( $n = 6$ ). \* $P < 0.05$  vs. Ctrl; # $P < 0.05$  vs. TRPC3 WT rhabdo (two-way ANOVA, with Tukey post hoc test); bar = 100  $\mu\text{m}$ .

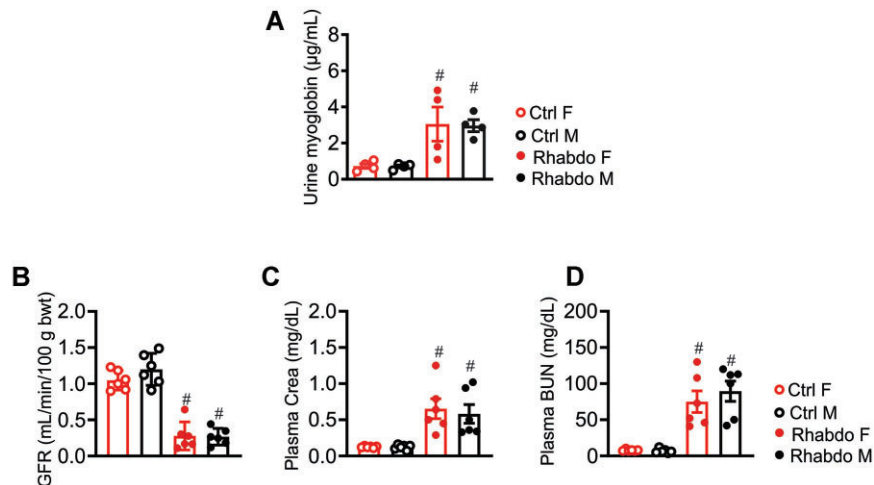


**Figure 10.** Twenty-four-hour rhabdomyolysis causes comparable AKI in male and female rats. (A) Urine myoglobin levels in saline (Ctrl)- and glycerol (Rhabdo)-treated male (M) and female (F) rats ( $n = 4$ ). (B–D) Twenty-four-hour GFR, plasma creatinine, and BUN in Ctrl and Rhabdo M and F rats ( $n = 6$ ). # $P < 0.05$  vs. Ctrl (two-way ANOVA, with Tukey post hoc test).

Trappani and colleagues demonstrated CGS 35066's selectivity and near-total efficacy in blocking ET-1-induced elevation in MAP.<sup>26</sup> Bosentan, a double  $\text{ET}_A/\text{ET}_B$  receptor antagonist, has been shown to inhibit the pressor response to ET-1 for up to 24 h at 100 mg/kg.<sup>25</sup> Similar doses have demonstrated therapeutic potential in animal models of acute lung injury, pulmonary

hypertension, and depression, principally via ET-1 antagonism.<sup>59–61</sup> Post-injury administration of Pyr3 improved neurological indices following intracerebral hemorrhage in mice, primarily by inhibiting the thrombin-induced opening of TRPC3 channels and  $\text{Ca}^{2+}$  influx in astrocytes.<sup>62</sup> In selecting the pharmacological agents, we targeted the upstream and downstream

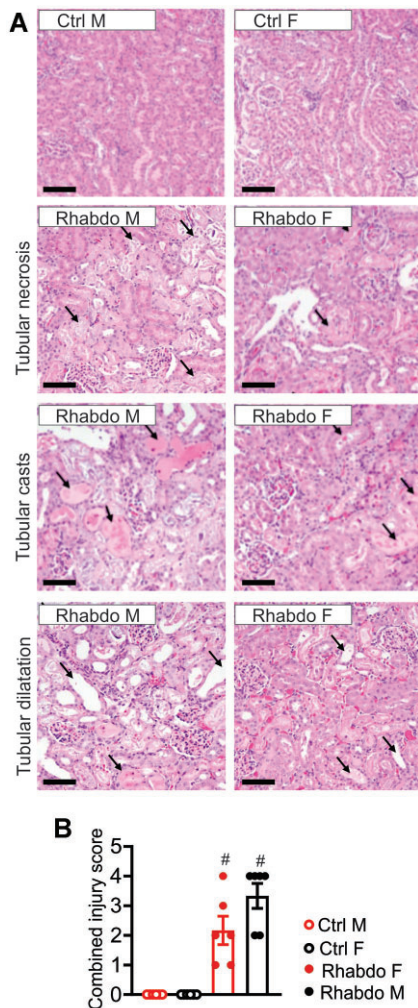


**Figure 11.** Histopathology indicates that rhabdomyolysis causes comparable kidney damage in male and female rats. (A) Hematoxylin and eosin staining of kidney sections (arrows indicate tubular injury) and (B) combined injury score in saline (Ctrl)- and glycerol (Rhabdo)-treated male (M) and female (F) rats ( $n = 6$  each).  $^{\#}P < 0.05$  vs. Ctrl (two-way ANOVA, with Tukey post hoc test); bar = 100  $\mu\text{m}$ .

signaling involved in ET-1-dependent renal vasoregulation to provide clinically relevant therapies.

A limitation of most pharmacological modulators of ion channels is non-selectivity. To strengthen pharmacological data on the involvement of TRPC3 channels in rhabdomyolysis-induced AKI, TRPC3 mutant rats were used. Since the rats were generated on Dahl SS background, we examine baseline arterial pressure and renal injury indices in the rats. Six-week-old TRPC3 WT and KO fed a regular low-salt diet showed comparable MAP, GFR, heart rate, and plasma creatinine levels. However, ET-induced cation currents, renal artery contraction, increase in acute MAP and RVR, and renal hypoperfusion were all lessened in the KO rats. Rhabdomyolysis-induced AKI was also significantly diminished in TRPC3 KO rats, confirming for the first time, using pharmacological and genetic approaches, that the ET-1-TRPC3 nexus is involved in kidney hypoperfusion and injury following rhabdomyolysis.

There are significant sex differences in the etiology, pathophysiology, and outcomes of cardiovascular and kidney diseases.<sup>63-66</sup> Several animal studies demonstrate sexual dimorphism in the degree of kidney injury following ischemia,

with the female sex confirmed as a renoprotective variable in ischemic AKI.<sup>67-71</sup> Glomerular filtration rate is a sensitive indicator of renal insufficiency in exertional rhabdomyolysis.<sup>72</sup> Amorim et al. found that although males exhibited more significant creatine kinase activity post-exercise than females, GFR reduction showed no differences across sexes.<sup>73</sup> A literature search revealed that sex-dependent variability had not been established in glycerol-induced rhabdomyolysis. Here, there were no significant differences in glycerol-induced myoglobinuria (indicative of muscle damage), GFR reduction, and increases in plasma creatinine, BUN, and kidney damage in male compared with female rats, suggesting the lack of sex-dependent variation in rhabdomyolysis and AKI induced by glycerol.

In summary, the findings in this study suggest that ECE-1-driven ET-1 production and downstream activation of TRPC3-dependent vasoconstriction contribute to rhabdomyolysis-induced AKI. Hence, post-injury inhibition of ET-1-dependent vasoregulation may provide therapeutic targets for rhabdomyolysis-induced AKI.

## Acknowledgment

We thank Probetex, Inc. for the independent histological analysis.

## Author Contributions

Study conception and design: A.A. and J.M.A. Data acquisition: J.M.A., P.K., J.D.W., and R.K. Drafting of the manuscript: J.M.A. and A.A.

## Funding

The National Institutes of Health supported Dr. A. Adebisi under the award numbers R01 DK120595 and R01 HL151735. Dr. J.M. Afolabi was supported by the American Heart Association (AHA) Predoctoral Fellowship under award number 829872. The content of this publication is solely the authors' responsibility and does not necessarily represent the official views of the NIH and AHA. This project utilized resources provided by the Medical College of Wisconsin Genome Editing Rat Resource Center [supported by NIH grant: R24 HL114474 to Aron Geurts] and UAB-UCSD O'Brien Core Center for Acute Kidney Injury Research [NIH grant: P30 DK 079337].

## Conflict of Interest Statement

None.

## Data Availability

The data underlying this article will be shared on reasonable request to the corresponding author.

## References

1. Makris K, Spanou L. Acute kidney injury: definition, pathophysiology and clinical phenotypes. *Clin Biochem Rev* 2016;37(2):85-98.
2. Basile DP, Anderson MD, Sutton TA. Pathophysiology of acute kidney injury. *Compr Physiol* 2012;2(2):1303-1353.

3. Thomas ME, Blaine C, Dawney A, et al. The definition of acute kidney injury and its use in practice. *Kidney Int* 2015;**87**(1):62–73.
4. Khwaja A. KDIGO clinical practice guidelines for acute kidney injury. *Nephron Clin Pract* 2012;**120**(4):c179–c184.
5. Bellomo R, Ronco C, Kellum JA, Mehta RL, Palevsky P. Acute renal failure—definition, outcome measures, animal models, fluid therapy and information technology needs: the Second International Consensus Conference of the Acute Dialysis Quality Initiative (ADQI) Group. *Crit Care* 2004;**8**(4):R204–212.
6. Chertow GM, Burdick E, Honour M, Bonventre JV, Bates DW. Acute kidney injury, mortality, length of stay, and costs in hospitalized patients. *J Am Soc Nephrol* 2005;**16**(11):3365–3370.
7. Pickkers P, Darmon M, Hoste E, et al. Acute kidney injury in the critically ill: an updated review on pathophysiology and management. *Intensive Care Med* 2021;**47**(8):835–850.
8. Bosch X, Poch E, Grau JM. Rhabdomyolysis and acute kidney injury. *N Engl J Med* 2009;**361**(1):62–72.
9. Karam H, Bruneval P, Clozel JP, Loffler BM, Bariety J, Clozel M. Role of endothelin in acute renal failure due to rhabdomyolysis in rats. *J Pharmacol Exp Ther* 1995;**274**(1):481–486.
10. Petejova N, Martinek A. Acute kidney injury due to rhabdomyolysis and renal replacement therapy: a critical review. *Crit Care* 2014;**18**(3):224.
11. Esposito P, Estienne L, Serpieri N, et al. Rhabdomyolysis-associated acute kidney injury. *Am J Kidney Dis* 2018;**71**(6):A12–A14.
12. Gabow PA, Kaehny WD, Kelleher SP. The spectrum of rhabdomyolysis. *Medicine (Baltimore)* 1982;**61**(3):141–152.
13. Zager RA. Rhabdomyolysis and myohemoglobinuric acute renal failure. *Kidney Int* 1996;**49**(2):314–326.
14. Bonventre JV, Weinberg JM. Recent advances in the pathophysiology of ischemic acute renal failure. *J Am Soc Nephrol* 2003;**14**(8):2199–2210.
15. Shimizu T, Kuroda T, Ikeda M, Hata S, Fujimoto M. Potential contribution of endothelin to renal abnormalities in glycerol-induced acute renal failure in rats. *J Pharmacol Exp Ther* 1998;**286**(2):977–983.
16. Roubert P, Gillard-Roubert V, Pourmarin L, et al. Endothelin receptor subtypes A and B are up-regulated in an experimental model of acute renal failure. *Mol Pharmacol* 1994;**45**(2):182–188.
17. Pollock DM, Pollock JS. Endothelin and oxidative stress in the vascular system. *CVP* 2005;**3**(4):365–367.
18. Dammanahalli KJ, Sun Z. Endothelins and NADPH oxidases in the cardiovascular system. *Clin Exp Pharmacol Physiol* 2008;**35**(1):2–6.
19. Lopez-Ongil S, Saura M, Zaragoza C, et al. Hydrogen peroxide regulation of bovine endothelin-converting enzyme-1. *Free Radical Biol Med* 2002;**32**(5):406–413.
20. Adebisi A, Thomas-Gatewood CM, Leo MD, Kidd MW, Neeb ZP, Jaggar JH. An elevation in physical coupling of type 1 inositol 1,4,5-trisphosphate (IP<sub>3</sub>) receptors to transient receptor potential 3 (TRPC3) channels constricts mesenteric arteries in genetic hypertension. *Hypertension* 2012;**60**(5):1213–1219.
21. Adebisi A, Zhao G, Narayanan D, Thomas-Gatewood CM, Bannister JP, Jaggar JH. Isoform-selective physical coupling of TRPC3 channels to IP<sub>3</sub> receptors in smooth muscle cells regulates arterial contractility. *Circ Res* 2010;**106**(10):1603–1612.
22. Mederos y Schnitzler M, Storch U, Meibers S, et al. Gq-coupled receptors as mechanosensors mediating myogenic vasoconstriction. *Embo j* 2008;**27**(23):3092–3103.
23. Sakai K, Omizo H, Togashi R, et al. Rhabdomyolysis-induced acute kidney injury requiring hemodialysis after a prolonged immobilization at home in 2 morbidly obese women: case reports with literature review. *Ren Replace Ther* 2020;**6**(1):30.
24. Lu M, Fang XX, Shi DD, et al. A selective TRPC3 inhibitor Pyr3 attenuates myocardial ischemia/reperfusion injury in mice. *Curr Med Sci* 2020;**40**(6):1107–1113.
25. Clozel M, Breu V, Gray GA, et al. Pharmacological characterization of bosentan, a new potent orally active nonpeptide endothelin receptor antagonist. *J Pharmacol Exp Ther* 1994;**270**(1):228–235.
26. Trapani AJ, Beil ME, Bruseo CW, De Lombaert S, Jeng AY. Pharmacological properties of CGS 35066, a potent and selective endothelin-converting enzyme inhibitor, in conscious rats. *J Cardiovasc Pharmacol* 2000;**36**(5 Suppl 1): S40–S43.
27. Schock-Kusch D, Xie Q, Shulhevich Y, et al. Transcutaneous assessment of renal function in conscious rats with a device for measuring FITC-sinistrin disappearance curves. *Kidney Int* 2011;**79**(11):1254–1258.
28. Pais GM, Chang J, Liu J, Scheetz MH. A translational rat model to assess glomerular function changes with vancomycin. *Int J Antimicrob Agents* 2022;**59**(5):106583.
29. Fanous MS, Afolabi JM, Michael OS, Falayi OO, Iwhiwhu SA, Adebisi A. Transdermal measurement of glomerular filtration rate in mechanically ventilated piglets. *J Vis Exp* 2022;**187**(e64413):1–17.
30. Soni H, Kaminski D, Gangaraju R, Adebisi A. Cisplatin-induced oxidative stress stimulates renal Fas ligand shedding. *Ren Fail* 2018;**40**(1):314–322.
31. Shih IM, Torrance C, Sokoll LJ, Chan DW, Kinzler KW, Vogelstein B. Assessing tumors in living animals through measurement of urinary beta-human chorionic gonadotropin. *Nat Med* 2000;**6**(6):711–714.
32. Mulvany MJ, Halpern W. Contractile properties of small arterial resistance vessels in spontaneously hypertensive and normotensive rats. *Circ Res* 1977;**41**(1):19–26.
33. Bridges LE, Williams CL, Pointer MA, Awumey EM. Mesenteric artery contraction and relaxation studies using automated wire myography. *J Vis Exp* 2011;**55**(e3119):1–5.
34. Griffiths K, Madhani M. The use of wire myography to investigate vascular tone and function. *Methods Mol Biol* 2022;**2419**:361–376.
35. Wenceslau CF, McCarthy CG, Earley S, et al. Guidelines for the measurement of vascular function and structure in isolated arteries and veins. *Am J Physiol Heart Circ Physiol* 2021;**321**(1):H77–H111.
36. Keltz E, Khan FY, Rhabdomyolysis MG. The role of diagnostic and prognostic factors. *Muscle Ligaments and Tendons J* 2013;**03**(04):303–312.
37. Kurtz TW, Maletz RM, Hsu CH. Renal cortical blood flow in glycerol-induced acute renal failure in the rat. *Circ Res* 1976;**38**(1):30–35.
38. Ayer G, Grandchamp A, Wyler T, Truniger B. Intrarenal hemodynamics in glycerol-induced myohemoglobinuric acute renal failure in the rat. *Circ Res* 1971;**29**(2): 128–135.
39. Venkatachalam MA, Rennke HG, Sandstrom DJ. The vascular basis for acute renal failure in the rat. Preglomerular and

- postglomerular vasoconstriction. *Circ Res* 1976;**38**(4):267–279.
40. Kohan DE. Endothelin synthesis by rabbit renal tubule cells. *Am J Physiol Renal Physiol* 1991;**261**(2 Pt 2):F221–F226.
  41. Kitamura K, Tanaka T, Kato J, Ogawa T, Eto T, Tanaka K. Immunoreactive endothelin in rat kidney inner medulla: marked decrease in spontaneously hypertensive rats. *Biochem Biophys Res Commun* 1989;**162**(1):38–44.
  42. Kumar R, Soni H, Afolabi JM, et al. Induction of reactive oxygen species by mechanical stretch drives endothelin production in neonatal pig renal epithelial cells. *Redox Biol* 2022;**55**:102394.
  43. Zager RA, Johnson AC, Andress D, Becker K. Progressive endothelin-1 gene activation initiates chronic/end-stage renal disease following experimental ischemic/reperfusion injury. *Kidney Int* 2013;**84**(4):703–712.
  44. Abassi ZA, Tate JE, Golomb E, Keiser HR. Role of neutral endopeptidase in the metabolism of endothelin. *Hypertension* 1992;**20**(1):89–95.
  45. Janas J, Sitkiewicz D, Januszewicz A, Szczesniak C, Grenda R, Janas RM. Endothelin-1 inactivating peptidase in the human kidney and urine. *J Hypertens* 2000;**18**(4):475–483.
  46. Plotnikov EY, Chupyrkina AA, Pevzner IB, Isaev NK, Zorov DB. Myoglobin causes oxidative stress, increase of NO production and dysfunction of kidney's mitochondria. *Biochim Biophys Acta* 2009;**1792**(8):796–803.
  47. Hughes AK, Stricklett PK, Padilla E, Kohan DE. Effect of reactive oxygen species on endothelin-1 production by human mesangial cells. *Kidney Int* 1996;**49**(1):181–189.
  48. Arendshorst WJ, Thai TL. Regulation of the renal microcirculation by ryanodine receptors and calcium-induced calcium release. *Curr Opin Nephrol Hypertens* 2009;**18**(1):40–49.
  49. Pollock DM, Jenkins JM, Cook AK, Imig JD, Inscho EW. L-type calcium channels in the renal microcirculatory response to endothelin. *Am J Physiol Renal Physiol* 2005;**288**(4):F771–F777.
  50. Fellner SK, Arendshorst W. Endothelin-A and -B receptors, superoxide, and Ca<sup>2+</sup> signaling in afferent arterioles. *Am J Physiol Renal Physiol* 2007;**292**(1):F175–F184.
  51. Berridge MJ. Inositol trisphosphate and calcium signalling. *Nature* 1993;**361**(6410):315–325.
  52. Narayanan D, Adebisi A, Jaggar JH. Inositol trisphosphate receptors in smooth muscle cells. *Am J Physiol Heart Circ Physiol* 2012;**302**(11):H2190–H2210.
  53. Parekh AB, Putney JW, Jr. Store-operated calcium channels. *Physiol Rev* 2005;**85**(2):757–810.
  54. Sanders KM. Invited review: mechanisms of calcium handling in smooth muscles. *J Appl Physiol* 2001;**91**(3):1438–1449.
  55. McFadzean I, Gibson A. The developing relationship between receptor-operated and store-operated calcium channels in smooth muscle. *Br J Pharmacol* 2002;**135**(1):1–13.
  56. Putney JW. Physiological mechanisms of TRPC activation. *Pflugers Arch* 2005;**451**(1):29–34.
  57. Facemire CS, Mohler PJ, Arendshorst WJ. Expression and relative abundance of short transient receptor potential channels in the rat renal microcirculation. *Am J Physiol Renal Physiol* 2004;**286**(3):F546–F551.
  58. Battistini B, Ayach B, Molez S, Blouin A, Jeng AY. Effects of benazepril, an angiotensin-converting enzyme inhibitor, combined with CGS 35066, a selective endothelin-converting enzyme inhibitor, on arterial blood pressure in normotensive and spontaneously hypertensive rats. *Clin Sci (Lond)* 2002;**103**(s2002): 363S–366S.
  59. Araz O, Demirci E, Yilmazel Ucar E, et al. Comparison of reducing effect on lung injury of dexamethasone and bosentan in acute lung injury: an experimental study. *Multidiscip Respir Med* 2013;**8**(1):74.
  60. Hill NS, Warburton RR, Pietras L, Klinger JR. Nonspecific endothelin-receptor antagonist blunts monocrotaline-induced pulmonary hypertension in rats. *J Appl Physiol* 1997;**83**(4):1209–1215.
  61. Pinho-Ribeiro FA, Borghi SM, Staurengo-Ferrari L, Filgueiras GB, Estanislau C, Verri WA, Jr. Bosentan, a mixed endothelin receptor antagonist, induces antidepressant-like activity in mice. *Neurosci Lett* 2014;**560**:57–61.
  62. Munakata M, Shirakawa H, Nagayasu K, et al. Transient receptor potential canonical 3 inhibitor Pyr3 improves outcomes and attenuates astrogliosis after intracerebral hemorrhage in mice. *Stroke* 2013;**44**(7):1981–1987.
  63. Beale AL, Kaye DM, Marques FZ. The role of the gut microbiome in sex differences in arterial pressure. *Biol Sex Differ* 2019;**10**(1):22.
  64. Loutradis C, Pickup L, Law JP, et al. Acute kidney injury is more common in men than women after accounting for socioeconomic status, ethnicity, alcohol intake and smoking history. *Biol Sex Differ* 2021;**12**(1):30.
  65. Toth-Manikowski SM, Yang W, Appel L, et al. Sex differences in cardiovascular outcomes in CKD: findings from the CRIC study. *Am J Kidney Dis* 2021;**78**(2):200–209.e1.
  66. Neugarten J, Golestaneh L. Influence of sex on the progression of chronic kidney disease. *Mayo Clin Proc* 2019;**94**(7):1339–1356.
  67. Rodríguez F, Nieto-Cerón S, Fenoy FJ, et al. Sex differences in nitrosative stress during renal ischemia. *Am J Physiol Regul Integr Comp Physiol* 2010;**299**(5):R1387–R1395.
  68. Kher A, Meldrum KK, Wang M, Tsai BM, Pitcher JM, Meldrum DR. Cellular and molecular mechanisms of sex differences in renal ischemia-reperfusion injury. *Cardiovasc Res* 2005;**67**(4):594–603.
  69. Fekete A, Vannay A, Vér A, et al. Sex differences in heat shock protein 72 expression and localization in rats following renal ischemia-reperfusion injury. *Am J Physiol Renal Physiol* 2006;**291**(4):F806–F811.
  70. Hutchens MP, Fujiyoshi T, Komers R, Herson PS, Anderson S. Estrogen protects renal endothelial barrier function from ischemia-reperfusion in vitro and in vivo. *Am J Physiol Renal Physiol* 2012;**303**(3):F377–F385.
  71. Hutchens MP, Dunlap J, Hurn PD, Jarnberg PO. Renal ischemia: does sex matter? *Anesth Analg* 2008;**107**(1):239–249.
  72. Rojas-Valverde D, Sánchez-Ureña B, Crowe J, Timón R, Olcina GJ. Exertional rhabdomyolysis and acute kidney injury in endurance sports: a systematic review. *Eur J Sport Sci* 2021;**21**(2):261–274.
  73. Amorim MZ, Machado M, Hackney AC, de Oliveira W, Luz CP, Pereira R. Sex differences in serum CK activity but not in glomerular filtration rate after resistance exercise: is there a sex dependent renal adaptative response? *J Physiol Sci* 2014;**64**(1):31–36.